

# Post irradiation testing of samples from the irradiation experiments PARIDE 3 and PARIDE 4

M. Roedig <sup>a,\*</sup>, W. Kuehnlein <sup>a</sup>, J. Linke <sup>a</sup>, D. Pitzer <sup>a</sup>, M. Merola <sup>b</sup>,  
E. Rigal <sup>c</sup>, B. Schedler <sup>d</sup>, E. Visca <sup>e</sup>

<sup>a</sup> Forschungszentrum Juelich GmbH, EURATOM Association, D-52425 Juelich, Germany

<sup>b</sup> EFDA – CSU, D-85748 Garching, Germany

<sup>c</sup> CEA Grenoble, 17 Rue des Martyrs, F-38054 Grenoble cedex 9, France

<sup>d</sup> Plansee AG, Reutte, Austria

<sup>e</sup> Associazione EURATOM-ENEA sulla Fusione, C.R. Frascati, 00044 Frascati, Italy

## Abstract

In order to study the influence of fast neutrons on the behaviour of high heat flux components for ITER, miniaturized samples have been neutron irradiated. Neutron fluences were 0.2 dpa in carbon/0.15 dpa in tungsten (irradiation campaign PARIDE 3) and 1 dpa in carbon/0.6 dpa in tungsten (irradiation campaign PARIDE 4). Irradiation temperatures were 200 °C approximately for all samples. The irradiated mock-ups as well as un-irradiated reference samples were tested under thermal fatigue conditions by means of a high power electron beam facility. They were loaded up to several thousand cycles and later they were cut and investigated by hot metallography. In addition to these thermal fatigue experiments, the degradation of thermal conductivities for plasma facing materials has been investigated. Samples from CFCs and tungsten alloys have been tested. Thermal diffusivities were measured by a laser flash method, heat capacities by differential scanning calorimetry.

© 2004 Elsevier B.V. All rights reserved.

## 1. Introduction

The effect of fast neutrons is an important issue for the operation of plasma facing materials (PFMs) and components (PFCs) for ITER. In order to study the influence of such neutrons, the irradiation experiments PARIDE 1 and PARIDE 2 have been carried out in the mid of the nineties [1]. At that time beryllium was the main candidate material for the divertor and the first wall. But later, beryllium was replaced in divertor applications by carbon reinforced carbon materials (CFCs) and tungsten alloys. Therefore a new irradiation program has been launched which took into account the

demands of the new materials and new loading conditions. The new irradiation campaign consisted of two parts:

- PARIDE 3: temperature:  $\approx 200$  °C; cumulative dpa:  $\approx 0.2$  in carbon,  $\approx 0.15$  in tungsten,
- PARIDE 4: temperature:  $\approx 200$  °C; cumulative dpa:  $\approx 1.0$  in carbon,  $\approx 0.6$  in tungsten.

## 2. Testing of actively cooled mock-ups

### 2.1. Experimental details

Actively cooled divertor mock-ups consist of the plasma-facing material (CFC, W alloy) and a heat sink from CuCrZr. Several techniques are used for the joining process. Simulation of operational relevant loading conditions were performed by means of the electron

\* Corresponding author. Tel.: +49-2461 61 6383; fax: +49-2461 61 6435.

E-mail address: [m.roedig@fz-juelich.de](mailto:m.roedig@fz-juelich.de) (M. Roedig).

beam facility JUDITH located in a hot cell at FZJ [2]. Cooling during the tests was achieved by water of room temperature. The flow rate of cooling water was 12 m/s. Twisted tapes were used in order to improve the cooling effect.

In the case of CFC mock-ups, the power absorbed by the mock-ups during the test was determined by water calorimetry. But in the case of tungsten alloys this method over-estimates the power density and the absorbed power densities were calculated by multiplying the incident power densities with the absorption coefficient for tungsten of 55% [3].

Temperature distributions on the mock-up surface were controlled by an infra-red camera; a detachment of armor tiles is recognized as an increase of surface temperature. Additional pyrometers allowed the continuous supervision of surface temperatures during thermal fatigue tests.

## 2.2. CFC mock-ups

Two geometries of CFC mock-ups have been irradiated and tested (see Fig. 1(a) and (b)). Flat tile mock-ups consisted of the silicon doped CFC material NS31 [4]. Tiles were laser structured and joined to the CuCrZr heat sink by active metal casting (AMC) and electron beam welding [4].

Monoblock mock-ups were made from CFC material NB31. After drilling, the wall of the hole was laser structured and coated with copper by AMC technique. Then the CFC blocks were joined to the CuCrZr cooling tube by hot isostatic pressing.

In the unirradiated stage both types of mock-ups showed very high failure limits. The flat tile survived

1000 cycles at 11.5 and 20 MW/m<sup>2</sup> but it showed a progressive detachment of a tile at 23 MW/m<sup>2</sup>. The CFC monoblock was loaded for 1000 cycles at 19 MW/m<sup>2</sup>, but at a power density of 23 MW/m<sup>2</sup> the test had to be stopped after 700 cycles not because of a failure but because of the sublimation of the carbon due to the high surface temperatures. After neutron irradiation, both types of CFC mock-ups showed a dramatic increase of surface temperatures due to the reduced thermal conductivity (see Section 3.1). This proved to be a limiting factor for the testing of CFC mock-ups.

### 2.2.1. CFC flat tile mock-up

During steady state heating at a rather low power density of 1 MW/m<sup>2</sup>, the surface temperature increased from 155 °C for unirradiated specimens to 290 °C for the 0.2 dpa sample and 550 °C for the 1 dpa sample.

During thermal fatigue experiments at 15 MW/m<sup>2</sup> both samples did not show any indication of failure. But during the whole loading process of 1000 cycles the maximum surface temperature was slightly reduced due to annealing processes in the high temperature areas of the mock-ups (see Fig. 2).

For the sample irradiated at 0.2 dpa, detachment of a tile started after 200 cycles at 19.5 MW/m<sup>2</sup>. Testing of the sample irradiated at 1 dpa was limited to 15 MW/m<sup>2</sup> because the surface temperatures exceeded 2500 °C and erosion of the surface due to sublimation was observed.

### 2.2.2. CFC monoblock mock-up

After irradiation, the surface temperatures for this type of mock-up increased even more than for the flat tiles. The maximum surface temperature in a monoblock irradiated at 0.2 dpa increased from 401 to 1580 °C at a relatively moderate power density of 5 MW/m<sup>2</sup>.

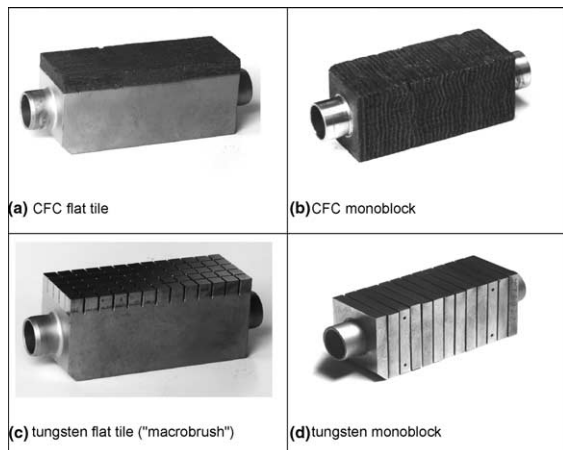


Fig. 1. Tested designs of divertor modules for ITER: (a) CFC flat tile; (b) CFC monoblock; (c) tungsten flat tile ('macrobrush'); (d) tungsten monoblock.

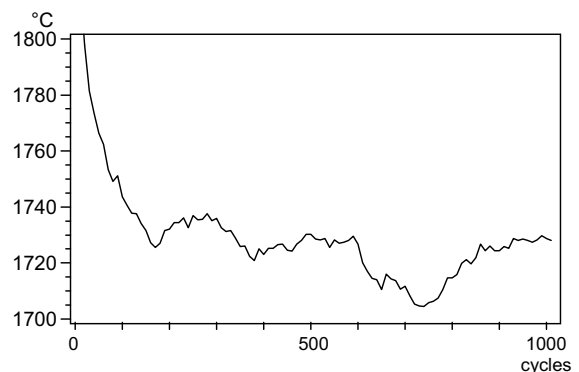


Fig. 2. Maximum surface temperature during thermal fatigue testing of an irradiated CFC flat tile mock-up at 15 MW/m<sup>2</sup> (irradiation condition: 0.2 dpa at 200 °C).

Thermal fatigue tests with this mock-up were carried out at  $10 \text{ MW/m}^2 \times 1000$  cycles and  $12 \text{ MW/m}^2 \times 1000$  cycles without failure. But when the power density level was increased to  $14 \text{ MW/m}^2$  heavy erosion occurred and no thermal cycling was possible. This again was not because of a failure of the sample but it was due to the high surface temperatures.

### 2.3. Tungsten mock-ups

Two basic designs of tungsten modules were involved in the PARIDE experiments (see Fig. 1(b) and (c)).

#### 2.3.1. Tungsten macrobrush mock-ups

Tungsten macrobrush mock-ups follow the flat tile design. They consist of small square shaped tiles of  $4 \times 4 \times 8 \text{ mm}^3$  made from W-1%La<sub>2</sub>O<sub>3</sub> which are coated on the lower side by OFHC copper and joined to the CuCrZr heat sink by electron beam welding.

Due to the high reflection of electrons in tungsten (45% compared to 5% in carbon), the maximum achievable power density on tungsten macrobrush mock-ups is  $14 \text{ MW/m}^2$  (absorbed). An unirradiated macrobrush mock-up did not show any indication of failure after 1000 cycles at 8 and  $14 \text{ MW/m}^2$ . After irradiation however, the failure limits are reduced to  $10 \text{ MW/m}^2$  approximately. Post mortem metallography shows a detachment of the tungsten rods at the border between W-1%La<sub>2</sub>O<sub>3</sub> and soft copper which is ascribed to an radiation induced embrittlement of the OFHC copper.

#### 2.3.2. Tungsten monoblocks

Tungsten monoblocks were manufactured by several producers with different designs. CEA and ENEA used W-1%La<sub>2</sub>O<sub>3</sub> tiles of 4 mm thickness which were joined to CuCrZr tubes by HIPing. The difference between the two designs was in HIPing temperature and pressure, as well as in the interlayers. A third type of mock-up was produced by Plansee; it consisted of thin tungsten lamellae of 0.2 mm. After drilling, the lamellae were covered by OFHC copper and in a second step they were joined to the CuCrZr tube by HIPing.

All unirradiated mock-ups were loaded at power densities between 14 and  $18 \text{ MW/m}^2$  but none of them showed any indication of failure during thermal cycling up to 1000 cycles at these power densities. Differently from the W macrobrush geometry, W monoblocks did not show any degradation of the fatigue performances even after irradiation and all survived 1000 cycles at  $18 \text{ MW/m}^2$ . Only one of the monoblocks was overheated at a screening even at a very low power density below  $3 \text{ MW/m}^2$ . But it is assumed that this was not due to irradiation effects but that the mock-up was faulty from the very beginning.

### 2.4. Summary of mock-up testing

All tested mock-ups are robust solutions and fulfill the requirements of the ITER divertor.

High heat flux testing with CFC mock-ups is limited by the high surface temperatures due to the degradation of thermal conductivities of carbon after irradiation. CFC flat tile mock-ups and tungsten macrobrush mock-ups show a slight reduction of failure limits after irradiation which is attributed to irradiation induced embrittlement of the OFHC Cu. CFC monoblock mock-ups do not show any failure up to the maximum achievable power density.

## 3. Thermal conductivity of irradiated samples

Thermal conductivity  $\lambda(T)$  can be calculated from the equation

$$\lambda(T) = \alpha(T)\rho(T)c_p(T)$$

with  $\alpha(T)$ , thermal diffusivity;  $\rho(T)$ , density;  $c_p(T)$ , heat capacity.

Thermal diffusivities were measured with a laser flash apparatus. In this method, a small disc shaped sample is loaded by a short laser pulse, and the resulting temperature increase on the back side of the sample is measured. From the slope of the temperature vs. time curve, thermal diffusivities are calculated.

Heat capacities were measured by means of a Netzsch differential scanning calorimeter DSC 404-C Pegasus [5]. In this apparatus, a small sample is loaded in a controlled heating cycle, and the temperature response of this sample is compared to the one of a reference sample. From the heat flux to and from the sample, thermophysical parameters (transition enthalpies, transition temperatures, heat capacities) can be deduced. In principle, measurements can be carried out between room temperature and  $1400 \text{ }^\circ\text{C}$ , but below  $150 \text{ }^\circ\text{C}$  the measured heat capacities are unreliable; and data for these temperatures were extrapolated.

### 3.1. CFC materials NB31 and NS31

Thermal conductivities have been determined for the 3D-CFC material SEPcarb NB31 and the corresponding silicon-doped material SEPcarb NS31, produced by Snecma Propulsion Solide [4].

Samples for thermal diffusivity measurements have been cut for the three main orientations of the CFCs. The same sets of samples have been measured before and after irradiation.

Heat capacities were measured in the unirradiated stage and for both irradiation conditions. Geometrical

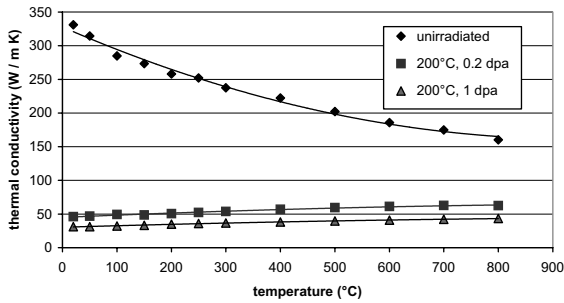


Fig. 3. Thermal conductivity of SEPCarb NB31 before and after irradiation (high conductivity direction).

densities were measured before and after irradiation with samples of 6 mm diameter and 25 or 30 mm length, respectively. The influence of temperature on the density has been neglected.

Fig. 3 shows the thermal conductivities for the high conductivity direction ( $x$ ) of the un-doped material NB31. As expected, the thermal conductivities are reduced significantly by the neutron irradiation. This reduction is mainly due to the degradation of thermal diffusivities, and it increases with the neutron dose. For all three directions, the room temperature conductivity is reduced to 10% after 1 dpa. This degradation takes place at a very early stage of the irradiation, as can be seen from the 0.2 dpa data in comparison to the 1 dpa data. At higher temperatures the effect of neutrons is lower, but even at the highest test temperature of 800 °C the thermal conductivities drop to 1/3 at 1 dpa compared to the unirradiated data.

The thermal conductivities for the silicone-doped material NS31 and their neutron-induced degradation are very similar to the ones of NB31.

### 3.2. Tungsten alloys

Pure tungsten and W-1%La<sub>2</sub>O<sub>3</sub> were tested in the unirradiated stage and after irradiation in the PARIDE 3 and PARIDE 4 campaigns. In addition thermal diffusivity samples from W-1%La<sub>2</sub>O<sub>3</sub> have been manufactured from used impact bending samples which had been irradiated in the former PARIDE 1 and PARIDE 2 irradiation experiments. The irradiation conditions for these samples were 0.2 dpa at 350 and 700 °C.

Samples for heat capacity measurements were also cut from used irradiated impact bending samples. According to [6] little swelling is observed for tungsten during irradiation. Therefore, the unirradiated heat capacities from literature were used as an input for the calculation of thermal conductivities.

The results for thermal conductivities of W-1%La<sub>2</sub>O<sub>3</sub> are shown in Fig. 4, the corresponding data for pure

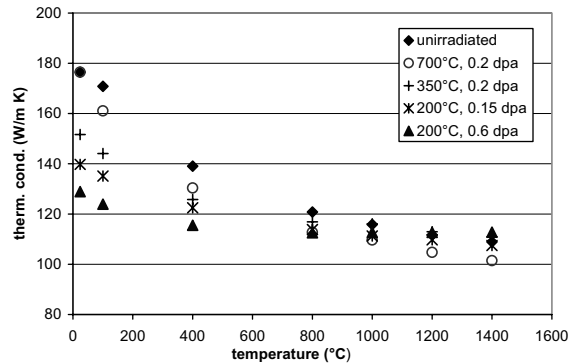


Fig. 4. Thermal conductivity of W-1%La<sub>2</sub>O<sub>3</sub> before and after irradiation.

tungsten are shown in [7]. Both materials show similar effects. The thermal diffusivity is decreased and the heat capacity is increased after neutron irradiation. However the effect on the thermal diffusivity is more distinct, and the latter gives a higher contribution to the degradation of thermal conductivity.

For temperatures below 800 °C, thermal conductivity is reduced with increasing neutron dose. But at higher irradiation temperatures annealing becomes effective, and the degradation is less serious.

## 4. Summary

The thermal conductivities are strongly reduced after neutron irradiation (especially for carbon). The degradation starts at a relatively low irradiation level and increases with the neutron dose. At higher temperatures the loss of thermal conductivities is less serious.

The failure limits of CFC flat tile and tungsten macrobrush mock-ups are slightly reduced after irradiation. This is especially valid for the tungsten macrobrush.

Due to its geometry, the monoblock design is a very robust solution for plasma facing components even after neutron irradiation.

## References

- [1] M. Rödig, R. Conrad, H. Derz, R. Duwe, J. Linke, A. Lodato, M. Merola, G. Pott, G. Vieider, B. Wiechers, *J. Nucl. Mater.* 283–287 (2000) 1161.
- [2] R. Duwe, W. Kühnlein, H. Münstermann, in: *Proceedings of the 18th Symposium on Fusion Technology (SOFT)*, Karlsruhe, Germany, 22–26 October 1994, p. 355.
- [3] M. Roedig, W. Kuehnlein, J. Linke, M. Merola, E. Rigal, B. Schedler, E. Visca, *Fus. Eng. Design* 61&62 (2002) S135.

- [4] M. Merola, Ch. Wu, in: 10th Carbon Workshop, Jülich, Germany, 17–19 September 2003.
- [5] Available from: <<http://www.ngb.netzsch.com/english/html/products/dsc/dsc404c.htm>>.
- [6] ITER Materials Properties Handbook, Version 2001.
- [7] A.T. Peacock, V Barabash, W. Dänner, M. Rödiger, P. Lorenzetto, P. Marmy, M. Merola, B. Singh, S. Tähtinen, J. van der Laan, Overview of recent European Materials R&D for ITER, *J. Nucl. Mater.*, these Proceedings. doi:10.1016/j.jnucmat.2004.04.008.